Bioorganic & Medicinal Chemistry 27 (2019) 3879–3888

Contents lists available at ScienceDirect

Bioorganic & Medicinal Chemistry

journal homepage: www.elsevier.com/locate/bmc

Discovery of fused bicyclic derivatives of 1*H*-pyrrolo[1,2-*c*]imidazol-1-one as VDR signaling regulators

Bin Xu[a,c], Mo-Yu Ding[b,c], Zhibing Weng[a], Zheng-Qing Li[b], Feng Li[a], Xia Sun[a], Qiu-Ling Chen[b], Yi-Tao Wang[b], Ying Wang[b,*,d], Guo-Chun Zhou[a,*,e]

[a] School of Pharmaceutical Sciences, Nanjing Tech University, Nanjing, Jiangsu 211816, China
[b] State Key Laboratory of Quality Research in Chinese Medicine and Institute of Chinese Medical Sciences, University of Macau, Avenida da Universidade, Taipa, Macao

ARTICLE INFO

Keywords:
1*H*-Pyrrolo[1,2-*c*]imidazol-1-one
vitamin D receptor (VDR)
Autophagy
Apoptosis

ABSTRACT

The modulation of VDR signaling is important in regulating tumor-related signal transduction and protecting from microorganismal infection. In this study we discovered by luciferase reporter assay that several fused bicyclic derivatives of 1*H*-pyrrolo[1,2-*c*]imidazol-1-one with the assistance of calcitriol result in up to three-fold increases of VDR promoter activity. Preliminary SAR results from 20 compounds disclose that ideal VDR signaling regulators of these compounds are built up by the optimal combination of multiple factors. Western blot analysis indicates that compounds of **ZD-3**, **ZD-4** and **ZD-5** not only significantly upregulate p62 and LC3-II but also elevate the ratio of LC3-II/LC3-I, which possibly leads to activated autophagy. All of five compounds also significantly downregulate p65 and upregulate p-p65 and **ZD-3** is the most active one to NF-κB signaling, suggesting a possible induction of apoptosis through the regulation of NF-κB signal transduction mediated by VDR signaling. Compounds of **ZD-3**, **ZD-4** and **ZD-5** significantly counteract the interference by VDR shRNA, in which **ZD-3** gets the highest compensation of VDR expression and the highest ratio of LC3-II/LC3-I, indicating that **ZD-3** very likely activates VDR-mediated autophagy. Taken together, these 1*H*-pyrrolo[1,2-*c*]imidazol-1-one derivatives can modulate VDR signaling, possibly resulting in the regulation of some signal pathways to induce autophagy and apoptosis.

1. Introduction

Vitamin D (VD) is a group of fat-soluble secosteroids and has been a powerful weapon for the treatment of rickets and osteomalacia since its first discovery in the 1920s–1930s. More broadly, VD is responsible for increasing the intestinal absorption of calcium, magnesium, and phosphate, and several other biological effects.[1] In humans, the most important compounds of VD are vitamin D_2 (VD2, ergocalciferol), vitamin D_3 (VD3, cholecalciferol), and 1,25-dihydroxycholecalciferol (calcitriol or abbreviated 1α,25-$(OH)_2D_3$, or 1,25-D3).[2] VD works as the natural ligand of the vitamin D receptor (VDR, also called calcitriol receptor), which is a ligand-dependent transcription factor and a member of the nuclear receptor family of transcription factors.[3] Activated VDR by VD undergoes a conformational change that promotes to form a heterodimer with the retinoid-X receptor (RXR) and then binds to hormone response elements on responsive gene DNA resulting in expression or transrepression of specific gene products. In addition to regulation of transcriptional responses, VDR is also involved in microRNA-directed post transcriptional mechanisms.[4]

VDR signaling has been taken as one of the most promising targets to battle against cancer, and some VDR ligands (agonists and antagonists or other modulators) have been demonstrated as anticancer agents.[5] It is proposed that the *VDR* gene is a determinant of survival in pancreatic cancer patients and plays a modulatory role of the VD pathway for the survival of advanced pancreatic cancer patients.[6] Multiple pre-clinical studies have demonstrated that calcitriol modulates normal mammary gland development and sensitivity to carcinogenesis, which imply calcitriol and its analogs anti-breast cancer potential.[7] A systematic review and network *meta*-analysis concluded that VDR genetic polymorphisms can be used to predict the transformation or prognosis of patients with breast cancer and ovarian cancer.[8] It is more important that dietary vitamin D supplementation in mice

* Corresponding authors.
E-mail addresses: emilyywang@umac.edu.mo (Y. Wang), gczhou@njtech.edu.cn (G.-C. Zhou).
[c] These authors contributed equally.
[d] ORCID: 0000-0002-1407-2668.
[e] ORCID: 0000-0003-3145-223X.

https://doi.org/10.1016/j.bmc.2019.07.024
Received 8 May 2019; Received in revised form 7 July 2019; Accepted 11 July 2019
Available online 12 July 2019

increases the basal levels of autophagy in the normal mammary gland, indicating the role of vitamin D and the VDR in modulating autophagy and the potential of vitamin D as a cancer-preventive agent.[9] Studies showed that vitamin D and the analog of EB 1089 can sensitize breast cancer cells to radiation through the promotion of a cytotoxic form of autophagy.[10] By contrast, calcitriol and EB 1089 enhance radiation sensitivity to non-small cell lung cancer (NSCLC) cells due to cytostatic autophagy induced by radiation in combination with either calcitriol or EB 1089.[11] Results from a randomized, double-blind, and placebo-controlled trial have suggested that vitamin D supplementation may improve the survival of NSCLC patients with early stage lung adenocarcinoma with lower calcitriol levels.[12]

As VD/VDR signaling promotes immune response, the signaling plays important role in protecting from infection by microorganism. Clinical outcomes of dengue virus (DENV) infection are associated with VDR gene polymorphisms and calcitriol reduces dengue virus infection in human cells.[13] Risk of HIV1 infection and rate of disease progression are also related with VDR polymorphism.[14a] It is revealed that some antiviral molecules correlated with VD/VDR signaling pathway genes are potentially participating in natural resistance to HIV-1.[14b] Deficiency of VD and decreased level of VDR were observed in patients with hepatitis C virus (HCV) and HCV-hepatocellular carcinoma (HCC) patients while a significant reduction in the serum concentration levels of microtubule-associated protein 1A/1B-light chain 3 (LC3) (a marker of autophagy) and caspase-3 (a marker of apoptosis) was referred to the downregulation of autophagy and apoptosis in HCV patients with or without HCC.[15] The relationship between VDR and inflammation reflects the pivotal association of VD/VDR signaling and inflammatory bowel disease (IBD).[16] Studies have found that VDR protein level is decreased in lungs of patients with chronic obstructive pulmonary disease (COPD) while dietary vitamin D may regulate epigenetic events, in particular on genes which are responsible for COPD susceptibility, and VD has also been implicated in reversal of steroid resistance and airway remodeling, which are the hallmarks of COPD and severe asthma.[17] Recent research indicates that VDR acts as a key modulator of inflammation and β cell survival and VDR ligand can promote VDR association important roles in potential protection of β cell for diabetes treatment.[18]

These findings demonstrate the pathogenic function of low VDR expression and VD/VDR signaling dysfunction observed in many diseases as well as their progression. Therefore, VDR ligands are becoming attractive therapeutics in many clinical fields and some VDR ligands have been biologically evaluated as drug candidates.[19] Although secosteroidal candidates exhibit efficient VDR activity in *in vitro* and *in vivo* studies, the secosteroidal skeleton exists some limitations due to their synthetic inconvenience, structural complexity, chemical instability, and potential hypercalcemia risk in clinical application. On the other hand, a lot of nonsecosteroidal skeleton vitamin D mimics[19,20] were designed and discovered in recent years as novel nonsecosteroidal VDR ligands, which possess low calcium mobilization and simple structures. Besides direct interaction between VDR and its specific ligand, a clinical drug of astemizole was discovered to synergize the antitumor effect of VD in HCC by inhibiting miR-125a-5p-meidated regulation of VDR,[21a] and the synergistic effect of bryostatin-1 with VD3 may play an important role in inducing the monocytic differentiation of NB4 acute promyelocytic leukemia cells.[21b]

In our previous study,[22a] **ZD-7**, **ZD-8** and **ZD-9** (Scheme 1), derivatives of 1*H*-pyrrolo[1,2-*c*]imidazol-1-one, as the fused bicyclic of pyrrolidine and 4-imidazolidinone, were demonstrated as NS2B-NS3 protease inhibitors of DENV-II and **ZD-7** is active against wild type DENV-II infection. In this study, we extend our exploration of structure–activity relationship (SAR) of these 1*H*-pyrrolo[1,2-*c*]imidazol-1-one derivatives. Our further study found that six new synthesized compounds and one known compound function regulatory activity of VDR signaling.

2. Results and discussion

2.1. Design and synthesis of new derivatives

In order to increase the diversity, furan and thiophene were introduced and different substituents at phenyl were explored. Furthermore, methenylene was inserted between the ring and phenyl for testing the flexibility of the basic scaffold. Dimer of 1*H*-pyrrolo[1,2-*c*]imidazol-1-one basic structure was explored to envisage possible extra binding to VDR signaling. Considering that methionine (Met) residue potentially increases the lipo- and hydro-solubility and also can improve the activity in previous report,[22b] Met residue was introduced. Among these structures, four compounds of **ZD-5**, **ZD-8**, **ZD-15** and **ZD-16** are alkyl acetals and others are aromatic acetals.

Nine known compounds of **ZD-7** to **ZD-15** were prepared previously.[22a] As shown in Scheme 1, nine new compounds of **ZD-1**, **ZD-2**, **ZD-5**, **ZD-6**, **ZD-16** to **ZD-19**, and **ZD-21** were synthesized modified from the previously reported procedure.[22a] Briefly, the condensation of Boc-L-proline with *p*-nitroaniline provided the first intermediate, which was followed by the deprotection of Boc group in the presence of trifluoroacetic acid (TFA) to yield the TFA salt of the second intermediate. Afterwards, in the catalysis of triethylamine (TEA), corresponding aldehydes reacted at 80 °C in toluene with the TFA salt to afford compounds of **ZD-1**, **ZD-2**, **ZD-5**, **ZD-6**, and **ZD-16** to **ZD-19**, and **ZD-21**, respectively. Among them, two dimers of **ZD-16** and **ZD-17** were prepared by 2.0 equivalent of the TFA intermediate with 1.0 equivalent of distinct dialdehyde. Furthermore, condensation of **ZD-6** with *N*-Boc-L-methionine gave the intermediate **ZD-20** and deprotection of Boc group of **ZD-20** by HCl (g) in ethyl acetate provided **ZD-3** as a hydrochloride salt; meanwhile, removal of Boc by HCl (g) in ethanol from **ZD-21** and then condensation with *N*-Boc-L-methionine by using isobutyl chloroformate (IBCF)[23] gave **ZD-4**. As we demonstrated before,[22a] the major isomers at C3-H and C7*a*-H of all these compounds (Scheme 1) are in *trans* configuration by comparison with the configuration of **ZD-10**, which was determined by the crystal structure (CCDC deposition number 1474483).

2.2. VDR signaling regulation and preliminary SAR

After compounds were synthesized, it was found that eleven new synthesized compounds of **ZD-1** to **ZD-6** and **ZD-16** to **ZD-20** are not active against DENV-II NS2B-NS3 protease (data not shown) as six known compounds of **ZD-11** to **ZD-15**, even though two known compounds **ZD-7** and **ZD-8** are DENV-II NS3-NS2B protease inhibitors and one known compound **ZD-9** is a weak NS2B-NS3 inhibitor.[22a] With these results, we turned our attention to revealing whether there is any interesting and important biological function of eleven new synthesized compounds and nine known compounds.[22a] Considering the importance of VDR signaling, VDR was selected as the first representative to test the activity of these compounds. HeLa cell lines stably harboring the luciferase reporter plasmid with VDR response elements[24] were constructed for the study. We utilized the luciferase reporter to examine the activity of eleven new compounds of **ZD-1** to **ZD-6** and **ZD-16** to **ZD-20** and also nine known compounds of **ZD-7** to **ZD-15** to VDR signaling pathway after their cytotoxicities (CC_{10}) to HeLa cells were firstly determined that none of these compounds show detectably cytotoxicity to HeLa cells with CC_{10} values of higher than 10 μM (Table S1 in Supplementary data).

It was discovered at first that all of these compounds alone are not obviously active to VDR (blue curves in Fig. 1, treatment with 0.1% DMSO vehicle control as background); however, it is interesting that the luciferase reporter expression is agonized/enhanced by **ZD-1** to **ZD-7** with 10 μM of each compound in a concentration-dependent manner when 200 nM of calcitriol was simultaneously applied (red curves in Fig. 1, treatment with calcitriol alone control as background). Whereas,

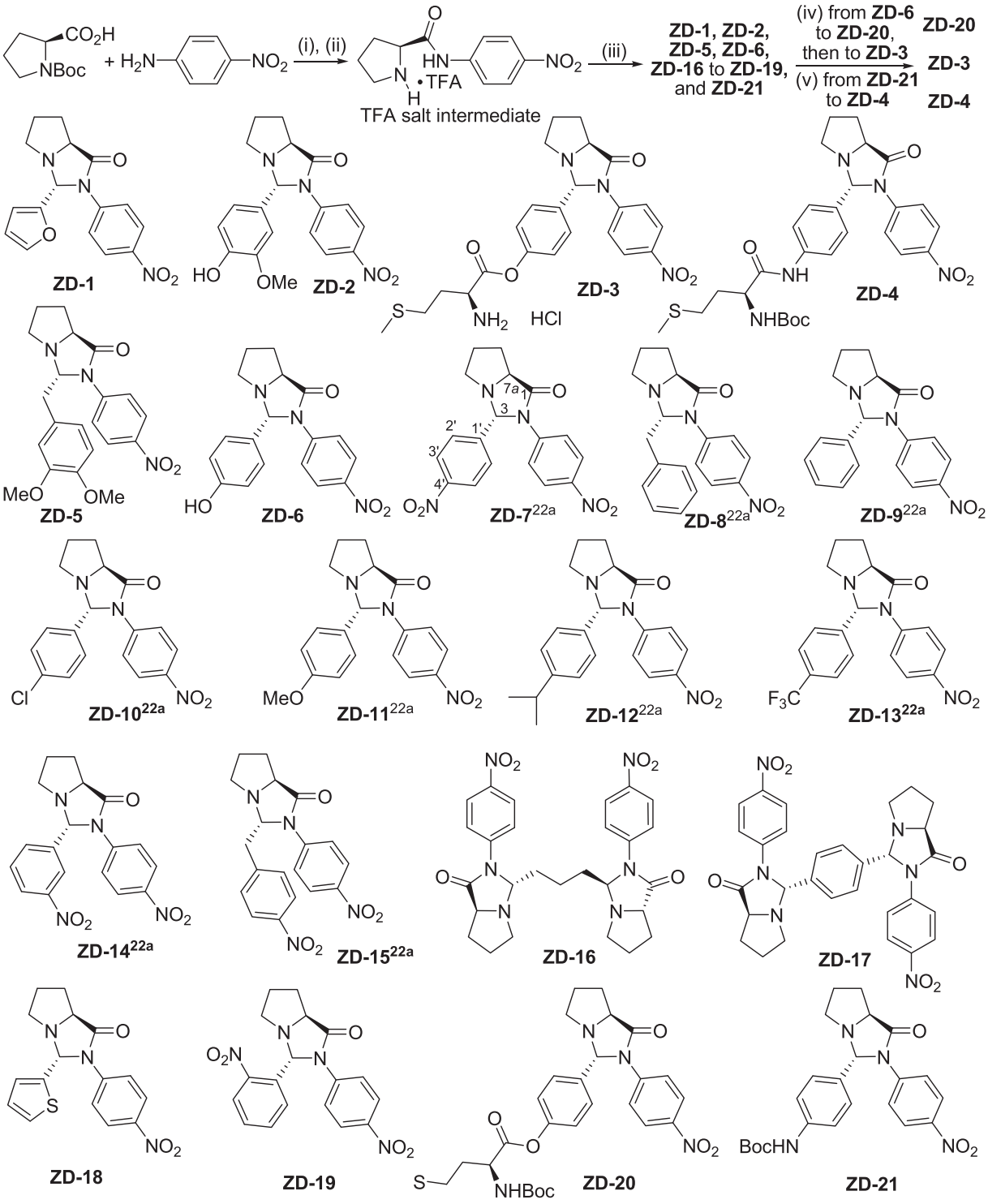

Scheme 1. Synthesis of 1*H*-pyrrolo[1,2-*c*]imidazol-1-one derivatives. Reagents and condition: (i) DCC, DMAP, anhydrous DCM, rt, 2 h. (ii) TFA, anhydrous DCM, 2 h. (iii) Aldehyde, TEA, 80 °C. (iv) (a) **ZD-6**, DCM, *N*-Boc-L-methionine, EDC, DMAP, rt, 2 h; (b) **ZD-20**, HCl (g) in EtOAc, 0 °C, 15 min. (v) (a) **ZD-21**, HCl (g) in EtOH, rt, 1.5 h; (b) DCM, TEA, *N*-Boc-L-methionine, IBCF, 0 °C, 12 h. (The position number in the compound refers to **ZD-7**.)

eight known compounds of **ZD-8** to **ZD-15** and five new compounds of **ZD-16** to **ZD-20** do not exhibit regulatory activity to VDR signaling in the experiments. These results (Fig. 1) suggest that this specific mode of action by these compounds of **ZD-1** to **ZD-7** may be achieved via their synergistic action with calcitriol to stimulate VDR activity, or/and their allosteric or/and direct binding to agonize VDR function. Among these VDR signaling regulators, compounds of **ZD-1** to **ZD-5** exhibit higher increment of VDR expression; whereas, **ZD-6** and known compound **ZD-7**[22a] induce relative lower enhancements of VDR promoter activity. Importantly, 10 μM of **ZD-3** or **ZD-5** gives rise to almost 2.5–3.0 fold increase of VDR promoter activity.

The structural difference between **ZD-1** and **ZD-18** is one atom by oxygen in furan and sulfur in thiophene, which makes **ZD-1** with furan be active VDR regulator but **ZD-18** bearing thiophene be inactive compound, possibly resulting from that furan can act as an acceptor of hydrogen-bond. Meanwhile, **ZD-6** with 4′-hydroxy phenyl is a weak

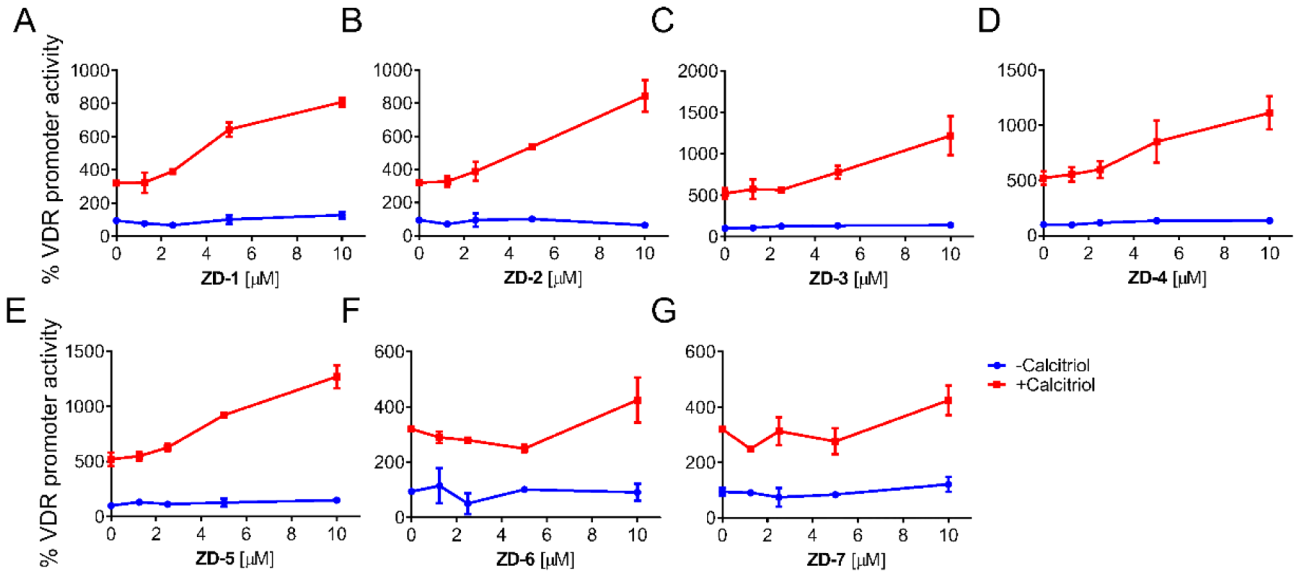

Fig. 1. The relative VDR promoter activity of compounds (A) **ZD-1**, (B) **ZD-2**, (C) **ZD-3**, (D) **ZD-4**, (E) **ZD-5**, (F) **ZD-6**, and (G) **ZD-7** in the presence (red curve, calcitriol alone control as background) or absence (blue curve, 0.1% DMSO control as background) of 200 nM calcitriol for 24 h. The results are presented as mean ± S.D. from at least three independent experiments. (Compounds of **ZD-1** to **ZD-6** are the new synthesized compounds while compound **ZD-7**[22a] is the known compound.)

VDR regulator but **ZD-9** without substitution at phenyl, **ZD-10** with 4′-chlorophenyl, and **ZD-11** bearing 4′-methoxy phenyl are inactive compounds, suggesting that 4′-hydroxyl group may play a role for **ZD-6** in regulating VDR signaling. Interestingly, **ZD-2** with one more 3-methoxy group is much more active VDR regulator than **ZD-6**. 4′-Nitrophenyl compound of **ZD-7** is a weak VDR signaling regulator but 3′-nitrophenyl compound of **ZD-14** and 2′-nitrophenyl compound of **ZD-19** are not active to VDR signaling. Moreover, **ZD-12** with 4′-*i*-Pr as a weak electron-donating group (EDG) and **ZD-14** with 4′-CF_3 as a strong electron-withdrawing group (EWG) do not exhibit VDR signaling regulation activity. Insertion of methylene linker at C3 position makes **ZD-5** become very active VDR regulator but makes **ZD-8** (an NS2B-NS3 protease inhibitor) and **ZD-15** be inactive to VDR signaling, indicating that alkyl acetal at C3 by methylene elongation can increase the activity and suitable substitution at benzyl is very important to VDR regulation. Meanwhile, VDR regulatory difference of two nitro compounds of **ZD-7** (a weak VDR regulator) and **ZD-15** (an inactive VRD regulator) suggests beneficial function of methylene linker depends on the substitution at arene. Two dimers of **ZD-16** and **ZD-17** are not active to VDR signaling, implying the extra recognition cannot establish by these dimers. It is noteworthy that introduction of Met residue is a valuable modification that ester **ZD-3** derived from phenol **ZD-6** is a very active VDR regulator and Boc-protected amide **ZD-4** prepared from **ZD-21** is also a good VDR regulator. Different from Boc-protected amide **ZD-4**, Boc-protected ester **ZD-20** is inactive VDR regulator, imply that amide bond and ester bond may affect the orientation of Met residue on the interaction with VDR signaling pathway. As summarized in Fig. 2, these preliminary SAR results show that the VDR regulatory activity of these compounds depends on optimal combination of arene feature, substituents at arene, side chain and distinct connection.

2.3. Western blot analysis of VDR signaling regulation by ZD-1 to ZD-5

With the understandings of VDR signaling regulation by these compounds, some key signaling factors associated with VDR by five potent compounds of **ZD-1** to **ZD-5** were studied in HeLa cells by Western blot (Fig. 3). First, the expression levels of p62 and LC3 connected with autophagy were examined. LC3 initially yields the cytosolic form LC3-I.[25] As such, LC3 and the ratio of LC3-II/LC3-I are considered to be crucial markers of autophagy and a higher LC3 II/I ratio indicates autophagy induction.[26] The protein p62 is an adaptor destined for consumption by the autophagosome machinery mediated possibly by ubiquitin–p62–LC3 interactions, and the upregulation/accumulation of p62 can be used as a marker of autophagosomal clearance.[27] Therefore, autophagy can be estimated by the observation of p62 and LC3. In comparison with two vehicle controls in the presence or absence of 200 nM of calcitriol, calcitriol alone does not obviously affect the expression levels of p62 and LC3. Based on the vehicle control with 200 nM calcitriol, p62 expression is significantly enhanced by treatment with 10 μM of all of five compounds. Among them, 10 μM of **ZD-2** or **ZD-4** is more active in activating p62 expression. The expression of LC3-II is significantly enhanced by 10 μM of all of five compounds while LC3-I expression is significantly enhanced by 10 μM of **ZD-1** to **ZD-4** but the enhancement by 10 μM of **ZD-5** is not significant. Importantly, the LC3-II/LC3-I ratios in the treatment with **ZD-3**, **ZD-4** and **ZD-5** are dramatically higher, which indicates possibly more activated autophagy. These results suggest that this series of compounds are able to induce autophagy.

NF-kappaB (NF-κB) are involved in the control of immune and inflammatory responses, developmental processes, cellular growth, and apoptosis; while incorrect regulation of NF-κB signal pathway is linked to cancer, inflammatory and autoimmune diseases, viral infection, and other related improper immune reactions. Importantly, evidences show that two signal pathways of VDR and NF-κB are sometimes interactive and cross-talking.[28] Moreover, the fact was observed that VDR and VD downregulate/inhibit NF-κB activity to induce apoptosis and autophagy.[29] Therefore, we were interested in Western blot results for the influences of these compounds on p65 and phospho-p65 (p-p65) of NF-κB signaling. As shown in Fig. 3, the expression of p65 is significantly decreased while that of p-p65 is notably enhanced by the application of 200 nM of calcitriol alone; meanwhile, the expression of p65 is significantly decreased while that of p-p65 is potently increased by the simultaneous application of 10 μM of these five compounds and 200 nM of calcitriol. Among these compounds, **ZD-3** reduces the lowest level of p65 and **ZD-2** increases the highest level of p-p65. Overall, these data indicate that calcitriol promotes the connection of these compounds

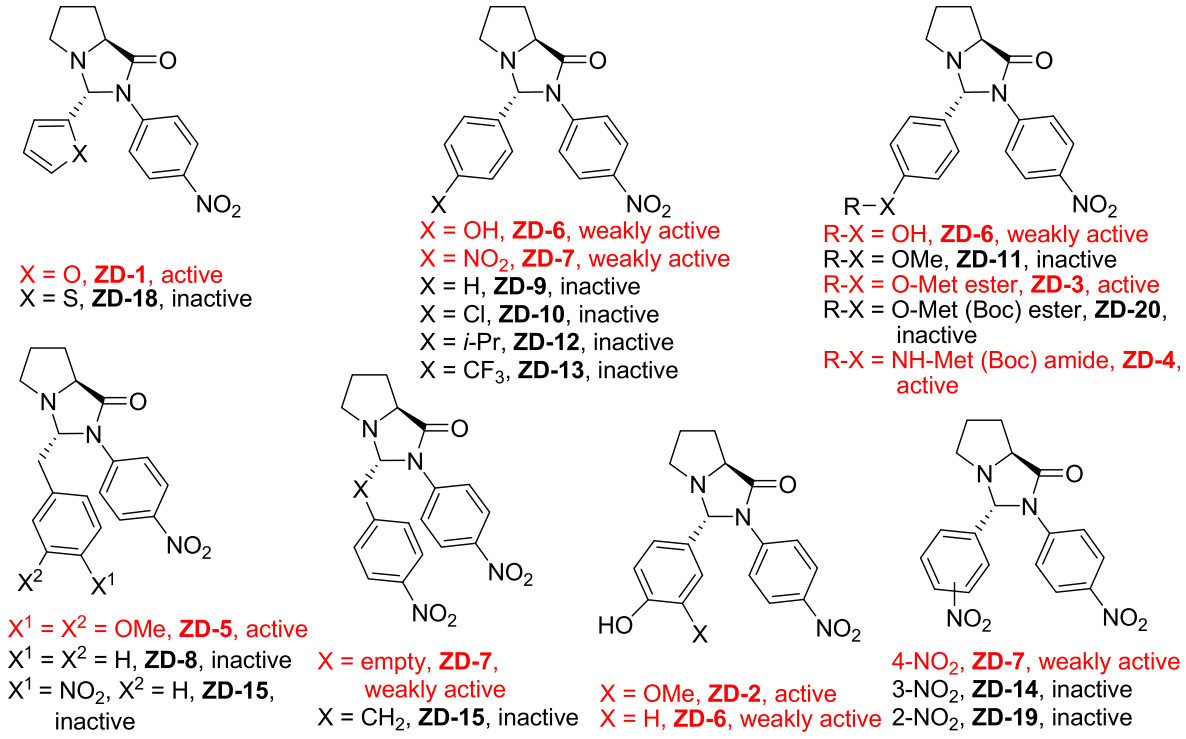

Fig. 2. The SAR summary of compounds in this study (two inactive dimmers of **ZD-16** and **ZD-17** are not included here; red highlights mean active compounds.

with NF-κB signaling and these compounds also can induce apoptosis through regulating NF-κB signal transduction mediated by VDR signaling.

2.4. Interference of VDR shRNA on VDR signaling regulation by these compounds

By using the interfering RNA technique (Fig. 4), we further investigated whether VDR signaling mediates the regulation of autophagy-related key factors of p62 and LC3. As expected, calcitriol significantly agonizes VDR while VDR shRNA significantly knocks down VDR. As predicted, calcitriol significantly rescues VDR from the knockdown by VDR shRNA even though the rescue cannot make full regain of VDR. In contrast to the activation of VDR, calcitriol almost does not affect p62 and LC3-I but slightly upregulates LC3-II. VDR shRNA knocks down VDR expression and the knockdown of VDR by its shRNA is partially but significantly counteracted by calcitriol. VDR shRNA considerably downregulates p62 and LC3-I, whereas the knockdown effect of VDR shRNA on p62 is not obviously affected by calcitriol while that on LC3-I is obvious but not significant. Moreover, VDR shRNA alone or calcitriol alone or their combination upregulates LC3-II but does not significantly affect LC3-II. Considering that HeLa cells undergo autophagy induced by Torin (an effective inducer of autophagy), the simultaneous application of Torin and VDR shRNA significantly downregulates VDR, p62 and LC3-I while obviously upregulates LC3-II. Furthermore, compared with the vehicle with calcitriol and VDR shRNA, compounds of **ZD-1** and **ZD-2** almost do not affect VDR expression by the interference of VDR shRNA; whereas three compounds of **ZD-3**, **ZD-4** and **ZD-5** significantly rescue VDR expression from the knockdown by VDR shRNA. This finding indicates that **ZD-3**, **ZD-4** and **ZD-5** increase the efficacy of the expression and function of VDR by specific mechanism/s. Compound **ZD-3** exhibits the highest activity among these compounds and even induces much higher VDR level than the vehicle with calcitriol agonist but without shRNA. However, p62 expression levels are not affected obviously by these compounds compared with the VDR shRNA vehicles with or without calcitriol. In comparison with the respective vehicle with calcitriol and VDR shRNA, all of five compounds upregulate LC3-I expression and the smaller increments are made by **ZD-3** and **ZD-5** but the higher increments are produced by **ZD-2** and **ZD-4**, while four compounds of **ZD-1** to **ZD-4** significantly upregulate but **ZD-5** downregulates LC3-II expressions. Among these, the highest ratio of LC3-II/LC3-I is made by **ZD-3**; hence, this result is at least in part parallel with the highest rescue by **ZD-3** of VDR expression from the interference of VDR shRNA. The decreasing order of LC3-II/LC3-I ratio is by **ZD-3**, **ZD-1**, **ZD-4**, **ZD-2** and **ZD-5**. Altogether, we can conclude that these compounds could interact with VDR signaling pathway by the distinct mechanism/s to significantly affect LC3 ratio and other key signals and subsequently to induce autophagy and apoptosis.

3. Conclusion

In this study, we discovered that the derivatives of 1*H*-pyrrolo[1,2-*c*]imidazol-1-one can modulate VDR signaling up to more than threefold augments with the assistance of calcitriol. Preliminary SAR results reveal that the VDR regulatory activity of these compounds depends on optimal combination of arene feature, substituents at arene, side chain and distinct connection. Western blot analyses indicate that five compounds of **ZD-1** to **ZD-5** significantly upregulate p62 and LC3-II, and three compounds of **ZD-3**, **ZD-4** and **ZD-5** exhibit the higher ratio of LC3-II/LC3-I, which suggests possibly higher activation of autophagy. In addition, five compounds significantly downregulate p65 and upregulate p-p65, suggesting there is possible induction of VDR-mediated apoptosis by regulating the NF-κB signal transduction. In accordance with above, **ZD-3** is the most active one to NF-κB signaling. The interfering study by VDR shRNA demonstrates that compounds of **ZD-3**, **ZD-4** and **ZD-5** significantly make up for the reduction of VDR expression knocked down by VDR shRNA, in which **ZD-3** obtains the highest compensation of VDR expression, followed by the induction of the highest ratio of LC3-II/LC3-I for autophagy. Considering that higher VDR augment is parallel to higher LC3-II and LC3-II/LC3-I ratio from the data, it implies that VDR signaling mediates the regulation of autophagy-related key factors of LC3-I and LC3-II. Hence, these compounds indeed have the regulatory functions on VDR and related factors

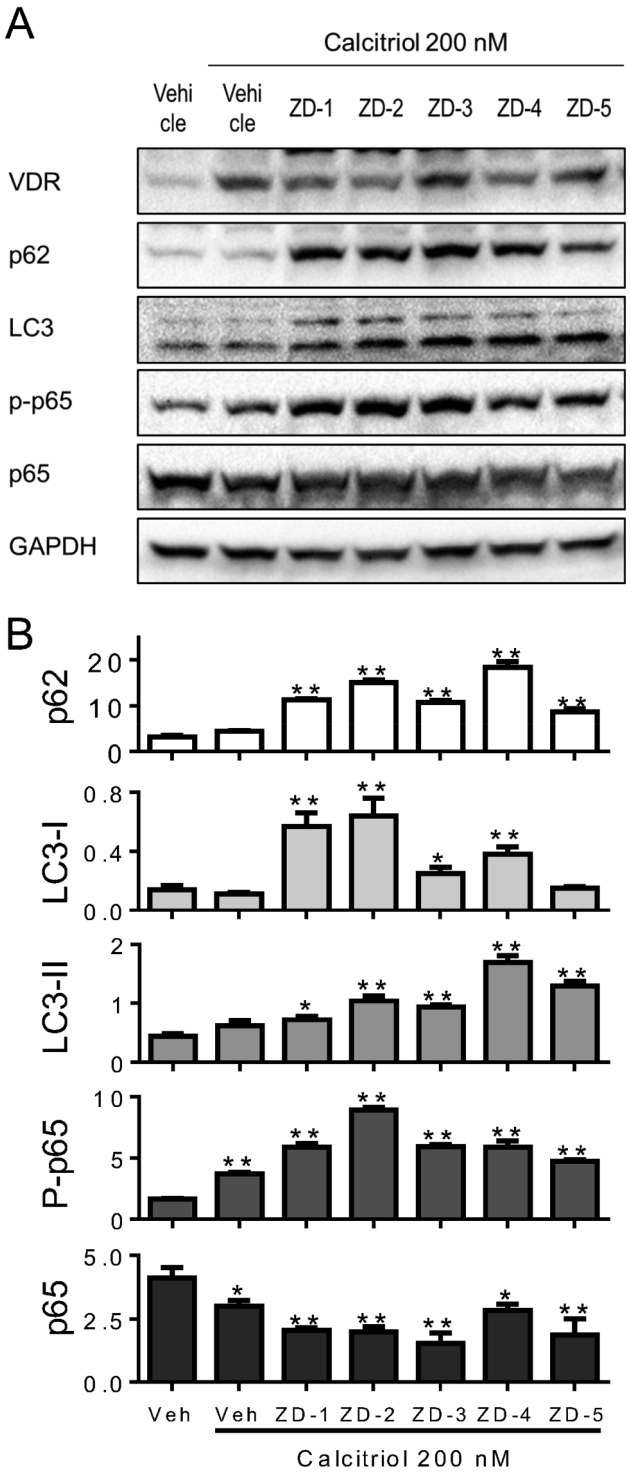

Fig. 3. (A) Expression level of p62, LC3, NF-κB p65 and p-p65 with the treatment of 10 μM of compounds of **ZD-1** to **ZD-5** in HeLa cells for 4 h. GAPDH blot was used as internal loading control. (B) Band intensity was normalized to that of GAPDH. The results are representatives of two separate experiments (**, $p < 0.05$; *, $p < 0.1$ compared with the vehicle treatment).

by synergistic, direct, or/and indirect/allosteric interaction, which exert some important effects on cellular life expectancy. Modulation of VDR signaling is important in regulating tumor-related signal transduction and protecting from microorganismal infection by immune response, therefore, the scaffold of 1*H*-pyrrolo[1,2-*c*]imidazol-1-one has a potential for anti-cancer treatment and anti-infection strategy. In conclusion, these results highlight the importance of these novel skeleton compounds and they can provide novel tools for insights into the role of VDR signaling in cancer and infectious diseases.

4. Materials and methods

4.1. General information for chemistry

^{1}H and ^{13}C NMR spectra were recorded on a Bruker AV-400 spectrometer at 400 and 100 MHz, respectively, in $CDCl_3$, CD_3OD, $(CD_3)_2SO$ and C_6D_6 as indicated. Coupling constants (J) are expressed in hertz (Hz). Chemical shifts (δ) of NMR are reported in parts per million (ppm) units relative to the solvent. The high resolution of ESI-MS was recorded on an Applied Biosystems Q-STAR Elite ESI-LC-MS/MS mass spectrometer, respectively. Unless otherwise noted, materials were obtained from commercial suppliers and used without further purification. Melting points were measured using an YRT-3 melting point apparatus (Shanghai, China) and were uncorrected. HPLC conditions for analysis of the purity of **ZD-1** to **ZD-6**: Sunfire C18 column (4.6 × 250 mm, 5 μm), elution by 60% acetonitrle with 40% purified water, rate = 1.0 mL/min, detection wavelength of 220 nm.

4.2. General preparation for compounds of *ZD-1, ZD-2, ZD-5, ZD-6, ZD-16 to ZD-19, and ZD-21*

The synthesis is modified from the published procedures.[22a] The TFA salt intermediate (250 mg, 0.9 mmol) was dissolved in 10 mL acetonitrile, then corresponding aldehyde (1.1 mmol, 1.2 equiv) and 0.2 mL triethylamine (1.4 mmol, 1.5 equiv) were added to the solution. The reaction mixture was stirred at 70 °C for 2 h. Upon completion, the reaction mixture was diluted with ethyl acetate (100 mL), the resulting solution was washed with water (50 mL), saturated aqueous $NaHCO_3$ solution (100 mL) and brine (50 mL), then dried over anhydrous Na_2SO_4, and filtered. The solvent is removed *in vacuo* to give the crude product. The residue was further purified by column chromatography on silica gel to give **ZD-1**, **ZD-2**, **ZD-5**, **ZD-6**, **ZD-16** to **ZD-19**, and **ZD-21**.

4.2.1. (3R,7aS)-3-(Furan-2-yl)-2-(4-nitrophenyl)hexahydro-1H-pyrrolo [1,2-c]imidazol-1-one (ZD-1)

40% yield, white solid, m.p. 142.0–143.0 °C. ^{1}H NMR (400 MHz, Methanol-d_4) δ 8.22 (d, J = 9.4 Hz, 2H), 7.88 (d, J = 9.4 Hz, 2H), 7.48 (dd, J = 1.8, 0.8 Hz, 1H), 6.44 (d, J = 3.3 Hz, 1H), 6.36 (dd, J = 3.3, 1.9 Hz, 1H), 6.27 (s, 1H), 4.19 (dd, J = 9.1, 4.2 Hz, 1H), 3.45–3.37 (m, 1H), 2.91 (m, 1H),2.33–2.20 (m, 1H), 2.20–2.12 (m, 1H), 1.94–1.84 (m, 2H); ^{13}C NMR (101 MHz, Methanol-d_4) δ 177.0, 152.4, 145.6, 144.6, 144.3, 125.5, 121.9, 111.5, 109.9, 77.5, 66.1, 56.2, 28.6, 25.6; HRMS (ESI) m/z found 314.1138 $[M+H]^+$, calculated for $C_{16}H_{16}N_3O_4$ 314.1141. The purity analyzed by HPLC is higher than 98%.

4.2.2. (3R,7aS)-3-(4-hydroxy-3-methoxyphenyl)-2-(4-nitrophenyl) hexahydro-1H-pyrrolo-[1,2-c]imidazol-1-one (ZD-2)

53% yield, white solid, m.p. 187.0–189.0 °C. ^{1}H NMR (400 MHz, DMSO-d_6) δ 9.06 (s, 1H), 8.20 (d, J = 9.3 Hz, 2H), 7.85 (d, J = 9.3 Hz, 2H), 6.90 (d, J = 1.6 Hz, 1H), 6.67 (d, J = 8.1 Hz, 1H), 6.62 (dd, J = 8.1, 1.9 Hz, 1H), 6.08 (s, 1H), 4.02 (dd, J = 9.0, 4.1 Hz, 1H), 3.72 (s, 3H), 3.28–3.24 (m, 1H), 2.82 (m, 1H), 2.12–2.04 (m, 1H), 2.01–1.95 (m, 1H), 1.85–1.76 (m, 1H), 1.75–1.67 (m, 1H); ^{13}C NMR (101 MHz, DMSO-d_6) δ 175.4, 147.8, 146.6, 143.4, 142.9, 130.1, 124.5, 120.4, 118.4, 115.3, 110.8, 81.7, 63.7, 55.6, 55.0, 27.3, 24.3; HRMS (ESI) m/z found 370.1398 $[M+H]^+$, calculated for $C_{19}H_{20}N_3O_5$ 370.1403. The purity analyzed by HPLC is higher than 98%.

4.2.3. (3R,7aS)-3-(3,4-Dimethoxybenzyl)-2-(4-nitrophenyl)hexahydro-1H-pyrrolo[1,2-c]- imidazol-1-one (ZD-5)

68% yield, white solid, m.p. 152.0–153.0 °C. ^{1}H NMR (400 MHz, DMSO-d_6) δ 8.30 (d, J = 9.2 Hz, 2H), 8.02 (d, J = 9.3 Hz, 2H), 6.81 (d,

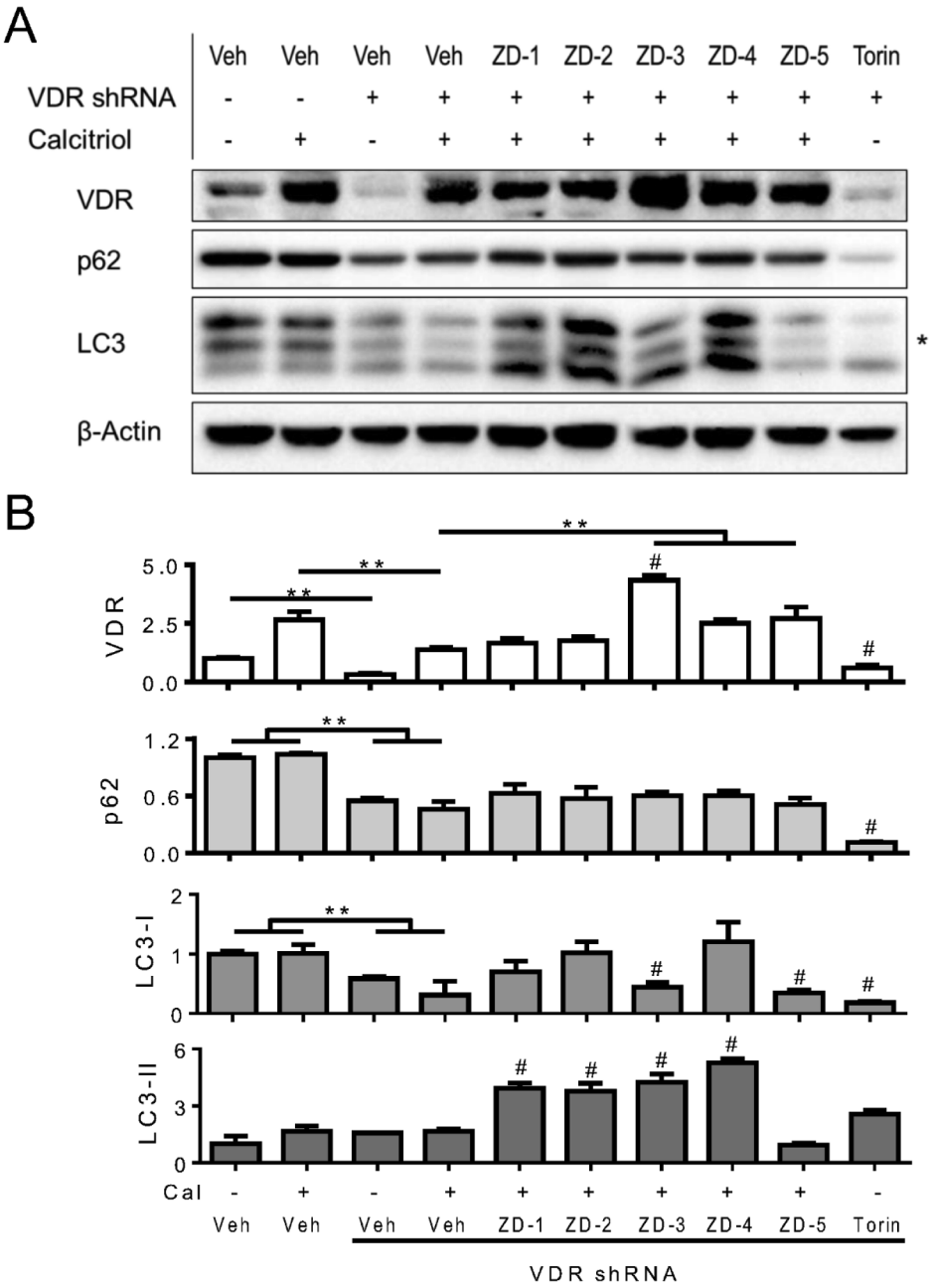

Fig. 4. (A) Expression levels of VDR, p62, and LC3 (upper band: LC3-I, lower band: LC3-II) were analyzed. HeLa cells were transiently transfected with VDR shRNA or control shRNA for 4 days prior to treatment. HeLa cells were then treated with 10 μM of **ZD-1** to **ZD-5** in combination with 200 nM calcitriol in HeLa cells for 4 h. Treatment with 100 nM of Torin 1 was used as positive control. β-Actin blot was used as internal loading control (*indicate non-specific band). (B) Band intensity was normalized to that of β-Actin. Results are representatives of two separate experiments (**, $p < 0.05$ between treatments; #, $p < 0.05$ to calcitriol treatment).

J = 8.7 Hz, 1H), 6.73–6.65 (m, 2H), 5.54 (dd, J = 5.8, 4.1 Hz, 1H), 3.69 (s, 3H), 3.67 (s, 3H), 3.53 (dd, J = 9.3, 4.2 Hz, 1H), 3.18–3.07 (m, 1H), 2.91–2.82 (m, 2H), 2.64 (m, 1H), 2.07–1.94 (m, 1H), 1.86–1.74 (m, 1H), 1.70–1.60 (m, 2H); ^{13}C NMR (101 MHz, DMSO-d_6) δ 175.5, 148.3, 147.6, 143.4, 142.9, 128.5, 124.8, 122.1, 120.4, 113.5, 111.6, 81.0, 64.2, 55.4, 55.2, 38.7, 27.3, 24.4; HRMS (ESI) *m/z* found 398.1709 $[M+H]^+$, calculated for $C_{21}H_{24}N_3O_5$ 398.1716. The purity analyzed by HPLC is higher than 98%.

4.2.4. (3R,7aS)-3-(4-Hydroxyphenyl)-2-(4-nitrophenyl)hexahydro-1H-pyrrolo[1,2-c] imidazol-1-one (ZD-6)

73% yield, white solid, m.p. 198.0–200.0 °C. ^{1}H NMR (400 MHz, DMSO-d_6) δ 9.51 (br s, 1H), 8.20 (d, J = 9.3 Hz, 2H), 7.85 (d, J = 9.3 Hz, 2H), 7.10 (d, J = 8.6 Hz, 2H), 6.69 (d, J = 8.5 Hz, 2H), 6.12 (s, 1H), 3.97 (dd, J = 9.1, 4.2 Hz, 1H), 3.27–3.23 (m, 1H), 2.81 (m, 1H), 2.14–2.04 (m, 1H), 2.01–1.92 (m, 1H), 1.83–1.76 (m, 1H), 1.73–1.65 (m, 1H); ^{13}C NMR (101 MHz, DMSO-d_6) δ 175.5, 157.3, 143.4, 142.9, 129.6, 127.6, 124.6, 120.3, 115.4, 81.5, 63.7, 54.9, 27.3, 24.3; HRMS (ESI) *m/z* found 362.1111 $[M+Na]^+$,calculated for $C_{18}H_{17}N_3NaO_4$ 362.1117. The purity analyzed by HPLC is higher than 95%.

4.2.5. (3R,3′R,7aS,7a'S)-3,3′-(propane-1,3-diyl)bis(2-(4-nitrophenyl) hexahydro-1H-pyrrolo [1,2-c]imidazol-1-one) (ZD-16)

45% yield, white solid, m.p. 101.9–102.8 °C. ^{1}H NMR (400 MHz, DMSO-d_6) δ 8.29–8.23 (m, 4H), 7.97–7.91 (m, 4H), 5.20 (d, J = 8.3 Hz, 2H), 4.00–3.96 (m, 2H), 3.16–3.06 (m, 2H), 2.68–2.58 (m, 2H), 2.15–2.02 (m, 2H), 1.89 (m, 2H), 1.76–1.48 (m, 10*H*); ^{13}C NMR

(101 MHz, DMSO- d_6) δ 175.0, 143.3, 142.9, 124.7, 120.2, 80.5, 64.0, 55.0, 32.9, 27.1, 24.4, 20.3; HRMS (ESI) *m/z* found 535.2300 $[M+H]^+$, calculated for $C_{27}H_{31}N_6O_6$, 535.2305.

4.2.6. (3R,3′R,7aS,7a'S)-3,3′-(1,4-phenylene)bis(2-(4-nitrophenyl) hexahydro-1H-pyrrolo [1,2-c] imidazol-1-one) (ZD-17)

40% yield, white solid, m.p. 157.4–158.2 °C. ^{1}H NMR (400 MHz, $CDCl_3$) δ 8.20–8.13 (m, 4H), 7.75–7.68 (m, 4H), 7.32 (s, 4H), 5.82 (s, 2H), 3.93 (t, J = 6.6 Hz, 2H), 3.52 (m, 2H), 2.90–2.80 (m, 2H), 2.26–2.16 (m, 4H), 1.98–1.85 (m, 4H); ^{13}C NMR (101 MHz, $CDCl_3$) δ 175.7, 143.7, 143.2, 139.0, 127.0, 124.9, 119.3, 82.1, 76.7, 63.9, 56.0, 27.2, 24.8; HRMS (ESI) *m/z* found 591.1963 $[M+Na]^+$, calculated for $C_{30}H_{28}N_6NaO_6$, 591.1968.

4.2.7. (3R,7aS)-2-(4-nitrophenyl)-3-(thiophen-2-yl)hexahydro-1H-pyrrolo [1,2-c]imidazol-1-one (ZD-18)

43% yield, white solid, m.p. 133.4–135.1 °C. ^{1}H NMR (400 MHz, $CDCl_3$) δ 8.27–8.17 (m, 2H), 7.84–7.76 (m, 2H), 7.30 (dd, J = 4.3, 2.0 Hz, 1H), 6.96–6.90 (m, 2H), 6.08 (s, 1H), 4.14 (dd, J = 8.9, 4.3 Hz, 1H), 3.55–3.45 (m, 1H), 2.88–2.78 (m, 1H), 2.34–2.15 (m, 2H), 2.02–1.87 (m, 2H); ^{13}C NMR (101 MHz, $CDCl_3$) δ 175.4, 143.9, 143.2, 142.5, 127.1, 126.4, 125.4, 124.8, 119.9, 78.8, 64.5, 55.2, 27.3, 24.9; HRMS (ESI) *m/z* found 330.0960 $[M+H]^+$, calculated for $C_{16}H_{16}N_3O_3S$, 330.0912.

4.2.8. (3R,7aS)-3-(2-nitrophenyl)-2-(4-nitrophenyl)hexahydro-1H-pyrrolo[1,2-c]imidazol-1-one (ZD-19)

50% yield, white solid, m.p. 163.4–164.7 °C. ^{1}H NMR (400 MHz, $CDCl_3$) δ 8.28–8.22 (m, 2H), 8.20–8.15 (m, 1H), 7.87–7.78 (m, 2H), 7.64–7.52 (m, 2H), 7.20–7.13 (m, 1H), 6.83 (s, 1H), 3.89 (s, 1H), 3.62 (s, 1H), 2.94 (m, 1H), 2.32–2.21 (m, 2H), 1.96 (q, J = 7.0, 6.1 Hz, 2H); ^{13}C NMR (101 MHz, $CDCl_3$) δ 176.6, 148.8, 143.8, 143.4, 133.5, 133.0, 129.9, 126.2, 126.0, 125.1, 118.7, 78.0, 63.9, 56.1, 27.2, 24.9; HRMS (ESI) *m/z* found 369.1195 $[M+H]^+$, calculated for $C_{18}H_{17}N_4O_5$, 369.1199.

4.2.9. tert-Butyl(4-((3R,7aS)-2-(4-nitrophenyl)-1-oxohexahydro-1H-pyrrolo[1,2-c]imidazol-3-yl)phenyl)carbamate (ZD-21)

77% yield, white solid, m.p. 86.0–88.0 °C. ^{1}H NMR (400 MHz, DMSO-d_6) δ 9.37 (s, 1H), 8.19 (d, J = 9.3 Hz, 2H), 7.84 (d, J = 9.3 Hz, 2H), 7.38 (d, J = 8.4 Hz, 2H), 7.19 (d, J = 8.6 Hz, 2H), 6.15 (s, 1H), 4.00 (dd, J = 9.1, 4.2 Hz, 1H), 3.28–3.23 (m, 1H), 2.84 (m, 1H), 2.14–2.05 (m, 1H), 2.03–1.94 (m, 1H), 1.84–1.77 (m, 1H), 1.73–1.67 (m, 1H), 1.44 (s, 9H); ^{13}C NMR (101 MHz, DMSO) δ 175.5, 152.7, 143.3, 143.0, 139.5, 132.8, 126.8, 124.6, 120.4, 118.2, 81.4, 79.2, 63.8, 55.1, 28.1, 27.3, 24.3; HRMS (ESI) *m/z* found 439.1978 $[M+H]^+$,calculated for $C_{23}H_{27}N_4O_5$ 439.1981.

4.3. Synthesis of ZD-20 and ZD-3 from ZD-6

4.3.1. 4-((3R,7aS)-2-(4-nitrophenyl)-1-oxohexahydro-1H-pyrrolo[1,2-c] imidazol-3-yl)- phenyl (tert-butoxycarbonyl)-L-methioninate (ZD-20)

To the solution of *N*-Boc-L-Methionine (200 mg, 0.8 mmol) and **ZD-6** (180 mg, 0.5 mmol) in anhydrous dichloromethane (5 mL), 1-(3-dimethylaminopropyl)-3-ethylcarbodiimide hydrochloride (EDCI) (120 mg, 0.6 mmol) and4-Dimethylaminopyridine (DMAP) (7 mg, 0.05 mmol) were added, then the reaction mixture was stirred at 25 °C for 2 h. After thatthe mixture was diluted with ethyl acetate (50 mL) and washed with water (50 mL), saturated aqueous $NaHCO_3$ (50 mL) and brine (50 mL), then dried over Na_2SO_4, and filtered. The solvent is removed under reduced pressure, the residue was further purified by column chromatography on silica gel to give 240 mg **ZD-20** as a white solid, 79% yield. m.p. 58.0–60.0 °C. ^{1}H NMR (400 MHz, DMSO-d_6) δ 8.21 (d, J = 9.3 Hz, 2H), 7.88 (d, J = 9.3 Hz, 2H), 7.54 (d, J = 7.4 Hz, 1H), 7.39 (d, J = 8.4 Hz, 2H), 7.07 (d, J = 8.4 Hz, 2H), 6.31 (s, 1H), 4.32–4.22 (m, 1H), 4.01 (dd, J = 9.1, 4.2 Hz, 1H), 3.32–3.24 (m, 1H), 2.87 (m, 1H), 2.63–2.53 (m, 2H), 2.18–2.05 (m, 1H), 2.05 (s, 3H), 2.03–1.93 (m, 3H), 1.83–1.76 (m, 1H), 1.75–1.67 (m, 1H), 1.38 (s, 9H); ^{13}C NMR (101 MHz, DMSO-d_6) δ 175.5, 171.3, 155.7, 150.2, 143.2, 143.1, 137.1, 127.7, 124.7, 121.9, 120.3, 80.9, 78.6, 63.7, 55.1, 52.8, 30.0, 29.6, 28.2, 27.3, 24.4, 14.5; HRMS (ESI) *m/z* found 593.2039 $[M+Na]^+$, calculated for $C_{28}H_{34}N_4NaO_7S$ 593.2046.

4.3.2. 4-((3R,7aS)-2-(4-nitrophenyl)-1-oxohexahydro-1H-pyrrolo[1,2-c] imidazol-3-yl)- phenyl L-methioninate hydrochloride (ZD-3)

Intermediate compound **ZD-20** (100 mg, 0.18 mmol) was dissolved in ethyl acetate (4 mL) and methyl *tert*-butyl ether (8 mL) in an ice bath, hydrogen chloride gas was passed through the solution and stirred for about 15 min. The resulting product was collected by filtration, washed by dichloromethane and dried under reduced pressure at 25 °C to afford **ZD-3**, 98% yield, white solid, m.p. 91.0–94.0 °C. ^{1}H NMR (400 MHz, Methanol-d_4) δ 8.26 (d, J = 9.2 Hz, 2H), 7.87 (d, J = 9.3 Hz, 2H), 7.74 (d, J = 8.6 Hz, 2H), 7.40 (d, J = 8.6 Hz, 2H), 6.80 (s, 1H), 4.91–4.85 (m, 1H), 4.54 (t, J = 6.3 Hz, 1H), 3.94–3.83 (m, 1H), 3.72–3.60 (m, 1H), 2.77 (t, J = 7.1 Hz, 2H), 2.49–2.37 (m, 3H), 2.37–2.27 (m, 1H), 2.25–2.19 (m, 1H), 2.15 (s, 3H), 2.13–2.07 (m, 1H); ^{13}C NMR (101 MHz, Methanol-d_4) δ 170.3, 169.0, 153.3, 146.3, 142.1, 132.6, 130.4, 125.7, 124.0, 123.3, 81.4, 65.3, 58.3, 52.9, 30.4, 30.0, 28.5, 25.3, 15.0; HRMS (ESI) *m/z* found 471.1696 $[M+H]^+$, calculated for $C_{23}H_{27}N_4O_5S$ 471.1702. The purity analyzed by HPLC is higher than 95%.

4.4. Synthesis of ZD-4 from ZD-21

4.4.1. (3R,7aS)-3-(4-aminophenyl)-2-(4-nitrophenyl)hexahydro-1H-pyrrolo[1,2-c]imidazol −1-one hydrochloride salt (intermediate)

Compound **ZD-21** (400 mg, 0.9 mmol) was dissolved in 10 mL ethyl acetate at 0 °C and then 2.7 mL hydrogen chloride-ethanol solution was dropped into the solution. After removing the ice bath, the reaction mixture was stirred at 25 °C for 1.5 h.The insoluble product was collected by filtration and then washed with ethyl acetate. Drying under reduced pressure for 6 h gave 310 mg amine hydrochloride salt intermediate as a pale yellow solid, 89% yield. m.p. 239.0–241.0 °C. ^{1}H NMR (400 MHz, Methanol-d_4) δ 8.23 (d, J = 9.3 Hz, 2H), 7.84 (d, J = 9.3 Hz, 2H), 7.80 (d, J = 8.6 Hz, 2H), 7.45 (d, J = 8.6 Hz, 2H), 6.94 (s, 1H), 5.05 (dd, J = 8.4, 5.2 Hz, 1H), 3.99 (m, 1H), 3.82 (m, 1H), 2.56–2.43 (m, 2H), 2.32–2.21 (m, 1H), 2.22–2.10 (m, 1H); ^{13}C NMR (101 MHz, Methanol-d_4) δ 168.6, 146.6, 141.5, 135.9, 133.0, 131.2, 125.7, 125.6, 123.6, 80.8, 65.3, 58.7, 28.5, 25.2; HRMS (ESI) *m/z* found 339.1461 $[M+H]^+$, calculated for $C_{18}H_{19}N_4O_3$ 339.1457.

4.4.2. tert-Butyl((S)-4-(methylthio)-1-((4-((3R,7aS)-2-(4-nitrophenyl)-1-oxohexahydro-1H-pyrrolo[1,2-c]imidazol-3-yl)phenyl)amino)-1-oxobutan-2-yl)carbamate (ZD-4)

To a stirred solution of *N*-Boc-L-Methionine (620 mg, 2.4 mmol) in anhydrous dichloromethane (10 mL) was slowly added triethylamine (0.4 mL, 3.0 mmol) at 0 °C. After 5 min, isobutyl chloroformate (IBCF) (0.35 mL, 2.7 mmol) was slowly added to the resulting mixture and stirred at 0 °C for 1 h. Then above amine hydrochloride salt (280 mg, 0.8 mmol) was added to the solution and the resulting mixture continued to stir at 0 °C for another 12 h. Upon completion, the mixture was diluted with ethyl acetate (50 mL) and washed with water (50 mL), saturated aqueous $NaHCO_3$ (50 mL) and brine (50 mL), then dried over anhydrous Na_2SO_4, and filtered. The solvent is removed under reduced pressure, the residue was further purified by column chromatography on silica gel to give 377 mg compound **ZD-4** as a white solid, 80% yield. m.p. 95.0–97.0 °C. ^{1}H NMR (400 MHz, DMSO-d_6) δ 10.03 (s, 1H), 8.20 (d, J = 9.3 Hz, 2H), 7.85 (d, J = 9.3 Hz, 2H), 7.54 (d, J = 8.5 Hz, 2H), 7.26 (d, J = 8.6 Hz, 2H), 7.14 (d, J = 7.8 Hz, 1H), 6.19 (s, 1H), 4.15–4.02 (m, 1H), 4.00 (dd, J = 9.1, 4.1 Hz, 1H), 3.29–3.24 (m, 1H), 2.90–2.79 (m, 1H), 2.49–2.37 (m, 2H), 2.16–2.03 (m, 1H), 2.03 (s, 3H), 2.04–1.92 (m, 1H), 1.88–1.76 (m, 3H), 1.74–1.66 (m, 1H), 1.36 (s, 9H);

^{13}C NMR (101 MHz, DMSO-d_6) δ 175.5, 171.0, 155.5, 143.3, 143.0, 138.9, 134.0, 126.8, 124.6, 120.3, 119.5, 81.3, 78.2, 63.8, 55.1, 54.4, 31.5, 29.8, 28.2, 27.3, 24.3, 14.7; HRMS (ESI) *m/z* found 592.2199 [M + Na]$^+$,calculated for $C_{28}H_{35}N_5NaO_6S$ 592.2206. The purity analyzed by HPLC is higher than 97%.

4.5. General information for biology

HeLa cell line was obtained from the American Type Culture Collection (ATCC). HeLa cells were maintained in DMEM high glucose medium supplemented with 10% FBS and 1% penicillin streptomycin. HeLa cells stably harboring VDR response element in pGL4.20 vector (Promega, Madison, WI, USA)[24] were maintained in the presence of 1 μg/mL puromycin. Calcitriol was purchased from Cayman Chemical. Fetal bovine serum (FBS) and penicillin streptomycin were purchased from Gibco.

All compounds were dissolved in DMSO before diluted with medium into stock solutions and the final concentration of DMSO in each well is 0.1%.

4.6. Construction of shRNA and transfection condition

The shRNA against human VDR was designed using the BioSETTIA shRNA designer and cloned into the pENTR^{TM}/H1/TO vector (Invitrogen). The sequence is as follows GCATGATGAAGGAGTT CATttggatccaaATGAACTCCTTCATCATGC (sense-loop-antisense). The shRNA plasmid was purified using endotoxin free HiPure Plasmid EF Mega Kit from Magen (Guangzhou, China), and transfected with TurboFect^{TM} Transfect reagent (ThermoFisher Scientific).

4.7. Western blot analysis

Western blot analysis was done using primary antibodies against p62 (Abcam #ab109012), LC3 (Cell Signaling Technology #12741), phospho-NF-κB-p65 (Cell Signaling Technology #3033), NF-κB-p65 (Cell Signaling Technology #8242), VDR (Cell Signaling Technology #12550), and GAPDH (Santa Cruz Biotechnology, #sc-32233) at optimal dilution.

4.8. VDR reporter assay

HeLa cells stably harboring luciferase reporter plasmids with VDR response element were used for the signaling pathway reporter assay.[24] Cells were treated with 200 nM Calcitriol to stimulate the corresponding downstream signaling pathways. Luciferase activity was measured using Luciferase assay kit (Promega) according to the manufacturer's instructions.

4.9. Cytotoxicity of testing compounds

HeLa cells were plated in a 96-well plate at a concentration of 1.0 x10^5 cells per well overnight to allow cell attachment. Working solutions of the testing compounds, or the 0.1% DMSO vehicle as a control were dispensed appropriately into the partitioned 96-well plates, which were then incubated for another 24 h. Then, the medium was discarded and the cells were incubated for 4 h at 37 °C in MTT solution (final concentration 0.5 mg/mL). The solution was then replaced with 100 mL DMSO to dissolve the violet formazan crystals in the intact cells. Cell growth was assessed by MTT according to the manufacturer's protocol. The absorbance was measured at 570 nm as the reference wavelength. The cytotoxicity as the CC_{10} value (concentration of 10% cell growth/viability inhibition) was calculated based on the percentage of cell viability data compared to the control group. Each concentration was repeated 3 times independently.

4.10. Statistical analysis

Data are presented as mean ± S.D. All experiments were repeated at least three times. Differences in measured variables between groups were analyzed by the student's *t* test by GraphPad Prism 5 software. Results were considered statistically significant when $p < 0.05$.

Declaration of Competing Interest

The authors declare that there are no conflicts of interest.

Acknowledgements

This work was partially supported by joint grant of National Natural Science Foundation of China and Macau Science and Development Fund FDCT 0004/2018/AFJ, FDCT 0013/2018/A, and Research Fund of the University of Macao MYRG2016-00105-ICMS-QRCM, MYRG2017-00116-ICMS-QRCM to YW. The work was also supported by the National Natural Science Foundation of China (30973621 and U0632001).

Appendix A. Supplementary data

Supplementary data (Table S1, HPLC spectra, and ^{1}HNMR and ^{13}C NMR spectra of new compounds) to this article can be found online at https://doi.org/10.1016/j.bmc.2019.07.024.

References

1. Holick MF. Sunlight and vitamin D for bone health and prevention of autoimmune diseases, cancers, and cardiovascular disease. *Am J Clin Nutr.* 2004;80:1678S–1688S.
2. Holick MF. High prevalence of vitamin D inadequacy and implications for health. *Mayo Clinic Proc.* 2006;81:353–373.
3. Moore DD, Kato S, Xie W, et al. International Union of Pharmacology. LXII. The NR1H and NR1I receptors: constitutive androstane receptor, pregnene X receptor, farnesoid X receptor alpha, farnesoid X receptor beta, liver X receptor alpha, liver X receptor beta, and vitamin D receptor. *Pharmacol Rev.* 2006;58:742–759.
4. Lisse TS, Chun RF, Rieger S, Adams JS, Hewison M. Vitamin D activation of functionally distinct regulatory miRNAs in primary human osteoblasts. *J Bone Miner Res.* 2013;28:1478–1488.
5. (a) Murray A, Madden SF, Synnott NC, et al. Vitamin D receptor as a target for breast cancer therapy. *Endocr Relat Cancer.* 2017;24:181–195
(b) Dou R, Ng K, Giovannucci EL, Manson JE, Qian ZR, Ogino S. Vitamin D and colorectal cancer: molecular, epidemiological and clinical evidence. *Br J Nutr.* 2016;115:1643–1660
(c) Chiang KC, Chen TC. The anti-cancer actions of vitamin D anticancer agents. *Med Chem.* 2013;13:126–139
(d) Hao M, Hou S, Xue L, et al. Further developments of the phenyl-pyrrolyl pentane series of nonsteroidal vitamin D receptor modulators as anticancer agents. *J Med Chem.* 2018;61:3059–3075.
6. Innocenti F, Owzar K, Jiang C, et al. The vitamin D receptor gene as a determinant of survival in pancreatic cancer patients: genomic analysis and experimental validation. *PLoS ONE.* 2018;13:e0202272.
7. JoEllen W. Vitamin D and breast cancer: past and present. *J Steroid Biochem Mol Biol.* 2018;177:15–20.
8. Li J, Li B, Jiang Q, et al. Do genetic polymorphisms of the vitamin D receptor contribute to breast/ovarian cancer? A systematic review and network meta-analysis. *Gene.* 2018;677:211–227.
9. Tavera-Mendoza LE, Westerling T, Libby E, et al. Vitamin D receptor regulates autophagy in the normal mammary gland and in luminal breast cancer cells. *Proc Natl Acad Sci USA.* 2017;114:E2186–E2194.
10. (a) Bristol ML, Di X, Beckman MJ, et al. Dual functions of autophagy in the response of breast tumor cells to radiation: cytoprtective autophagy with radiation alone and cytotoxic autophagy in radiosensitization by vitamin D3. *Autophagy.* 2012;8:739–753
(b) Wilson EN, Bristol ML, Di X, et al. A switch between cytoprotective and cytotoxic autophagy in the radiosensitization of breast tumor cells by chloroquine and vitamin. *Horm Cancer.* 2011;2:272–285.
11. Sharma K, Goehe RW, Di X, et al. A novel cytostatic form of autophagy in sensitization of non-small cell lung cancer cells to radiation by vitamin D and the vitamin D analog, EB 1089. *Autophagy.* 2014;10:2346–2361.
12. Akiba T, Morikawa T, Odaka M, Nakada T, Kamiya N, Yamashita M. Vitamin D supplementation and survival of patients with non-small cell lung cancer: a randomized, double-blind, placebo-controlled trial. *Clin Cancer Res.* 2014;24:4089–4097.
13. (a) Alagarasu K, Honap T, Mulay AP, Bachal RV, Shah PS, Cecilia D. Association of vitamin D receptor gene polymorphisms with clinical outcomes of dengue virus infection. *Hum Immunol.* 2012;73:1194–1199

(b) Dettogni RS, Tristão-Sá R, dos Santos M, da Silva FF, Louro ID. Single nucleotide polymorphisms in immune system genes and their association with clinical symptoms persistence in dengue-infected persons. *Hum Immunol.* 2015;76:717–723
(c) Alagarasu K, Bachal RV, Bhagat AB, Shah PS, Dayaraj C. Elevated levels of vitamin D and deficiency of mannose binding lectin in dengue hemorrhagic fever. *Virol J.* 2012;9:86
(d) Puerta-Guardo H, Medina F, De la Cruz Hernández SI, Rosales VH, Ludert JE, del Angel RM. The 1α,25dihydroxyvitamin D3 reduces dengue virus infection in human myelomonocyte (U937) and hepatic (Huh7) cell lines and cytokine production in the infected monocytes. *Antiviral Res.* 2012;94:57–61.
14. (a) Torres C, Sanchez de la Torre M, Garcia-Moruja C, et al. Immunophenotype of vitamin D receptor polymorphism associated to risk of HIV1 infection and rate of disease progression. *Curr HIV Res.* 2010;8:487–492
(b) Aguilar-Jimenez W, Zapata W, Rugeles MT. Antiviral molecules correlate with vitamin D pathway genes and are associated with natural resistance to HIV-1 infection. *Microbes Infect.* 2016;18:510–516.
15. Abdel-Mohsen MA, El-Braky AA, Ghazal AAE, Shamseya MM. Autophagy, apoptosis, vitamin D, and vitamin D receptor in hepatocellular carcinoma associated with hepatitis C virus. *Medicine.* 2018;97:e0172.
16. (a) Lim WC, Hanauer SB, Li YC. Mechanisms of Disease: vitamin D and inflammatory bowel disease. *Nat Clin Pract Gastroenterol Hepatol.* 2005;2:308–315
(b) Sentongo TA, Semaeo EJ, Stettler N, Piccoli DA, Stallings VA, Zemel BS. Vitamin D status in children, adolescents, and young adults with Crohn disease. *Am J Clin Nutr.* 2002;76:1077–1081
(c) Wu S, Zhang Y, Lu R, et al. Intestinal epithelial vitamin D receptor deletion leads to defective autophagy in colitis. *Gut.* 2015;64:1082–1094
(d) Liu W, Chen Y, Golan MA, et al. Intestinal epithelial vitamin D receptor signaling inhibits experimental colitis. *J Clin Invest.* 2013;123:3983–3996
(e) Del Pinto R, Ferri C, Cominelli F. Vitamin D axis in inflammatory bowel diseases: role, current uses and future perspectives. *Int J Mol Sci.* 2017;18:E2360
(f) Bakke D, Sun J. Ancient nuclear receptor VDR with new functions: microbiome and inflammation. *Inflamm Bowel Dis.* 2018;24:1149–1154
(g) Wu S, Sun J, Vitamin D. vitamin D receptor, and macroautophagy in inflammation and infection. *Discov Med.* 2011;11:325–335
(h) Wu S, Yoon S, Zhang YG, et al. Vitamin D receptor pathway is required for probiotic protection in colitis. *Am J Physiol Gastrointest Liver Physiol.* 2015;309:G341–G349.
17. (a) Chishimba L, Thickett DR, Stockley RA, Wood AM. The vitamin D axis in the lung: a key role for vitamin D-binding protein. *Thorax.* 2010;65:456–462
(b) Shaheen SO, Jameson KA, Robinson SM, Boucher BJ, Syddall HE, et al. Relationship of vitamin D status to adult lung function and COPD. *Thorax.* 2011;66:692–698
(c) Sundar IK, Rahman I. Vitamin d and susceptibility of chronic lung diseases: role of epigenetics. *Front Pharmacol.* 2011;2:50
(d) Pfeffer PE, Hawrylowicz CM. Vitamin D and lung disease. *Thorax.* 2012;67:1018–1020.
18. Wei Z, Yoshihara E, He N, et al. Vitamin D switches BAF complexes to protect β cells. *Cell.* 2018;173:1–15.
19. (a) Plum LA, DeLuca HF. Vitamin D, disease and therapeutic opportunities. *Nat Rev Drug Discov.* 2010;9:941–955
(b) Carlberg C, Molnar F. Current status of vitamin D signaling and its therapeutic applications. *Curr Top Med Chem.* 2012;12:528–547
(c) Belorusova AY, Rochel N. Modulators of vitamin D nuclear receptor: recent advances from structural studies. *Curr Top Med Chem.* 2014;14:2368–2377
(d) Yamada S, Makishima M. Structure-activity relationship of nonsecosteroidal vitamin D receptor modulators. *Trends Pharmacol Sci.* 2014;35:324–337
(e) Makishima M. Current topics on vitamin D. Nonsecosteroidal vitamin D mudulators and prospects for their thepapeutic application. *Clin Calcium.* 2015;25:403–411.
20. (a) Perakyla M, Malinen M, Herzig KH, Carlberg C. Gene regulatory potential of nonsteroidal vitamin D receptor ligands. *Mol Endocrinol.* 2015;19:2060–2073
(b) Boehm MF, Fitzgerald P, Zou A, et al. Novel nonsecosteroidal vitamin D mimics exert VDR-modulating activities with less calcium mobilization than 1,25-dihydroxyvitamin D3. *Chem Biol.* 1999;6:265–275
(c) Fujii S, Masuno H, Taoda Y, et al. Boron cluster-based development of potent nonsecosteroidal vitamin D receptor ligands: direct observation of hydrophobic interaction between protein surface and carborane. *J Am Chem Soc.* 2011;133:20933–20941
(d) Fujii S, Kano A, Masuno H, et al. Design and synthesis of tetraol derivatives of 1,12-dicarba-closo-dodecaborane as non-secosteroidal vitamin D analogs. *Bioorg Med Chem Lett.* 2014;24:4515–4519
(e) Fujii S, Kano A, Songkram C, et al. Synthesis and structure-activity relationship of p-carborane-based non-secosteroidal vitamin D analogs. *Bioorg Med Chem.* 2014;22:1227–1235
(f) Fujii S, Sekine R, Kano A, et al. Structural development of p-carborane-based potent non-secosteroidal vitamin D analog. *Bioorg Med Chem.* 2014;22:5891–5901.
21. (a) Xu J, Wang Y, Zhang Y, Dang S, He S. Astemizole promotes the anti-tumor effect of vitamin D through inhibiting miR-125a-5p-meidated regulation of VDR in HCC. *Biomed Pharmacother.* 2018;107:1682–1691
(b) Clark CS, Konyer JE, Meckling KA. 1α,25-dihydroxyvitamin D3 and bryostatin-1 synergize to induce monocytic differentiation of NB4 acute promyelocytic leukemia cells by modulating cell cycle progression. *Exp Cell Res.* 2004;294:301–311.
22. (a) Weng Z, Shao X, Graf D, et al. Identification of fused bicyclic derivatives of pyrrolidine and imidazolidinone as dengue virus-2 NS2B-NS3 protease inhibitors. *Eur J Med Chem.* 2017;125:751–759
(b) Zhou GC, Liu F, Wan J, et al. Discovery and SAR studies of methionine–proline anilides as dengue virus NS2B-NS3 protease inhibitors. *Bioorg Med Chem Lett.* 2013;23:6549–6554.
23. Franze'n HM, Bessidskaia G, Abedi V, Nilsson A, Nilsson M, Olsson L. Frakefamide, an analgesic tetrapeptide: development of a pilot-plant-scale process. *Org Process Res Dev.* 2002;6:788–797.
24. Ding N, Yu RT, Subramaniam N, et al. A vitamin D receptor/SMAD genomic circuit gates hepatic fibrotic response. *Cell.* 2013;153:601–613.
25. Wang W, Wang H, Geng QX, et al. Augmentation of autophagy by atorvastatin via Akt/mTOR pathway in spontaneously hypertensive rats. *Hypertens Res.* 2015;38:813–820.
26. (a) Deng Y, Wu W, Guo S, et al. Altered mTOR and Beclin-1 mediated autophagic activation during right ventricular remodeling in monocrotaline induced pulmonary hypertension. *Respir Res.* 2017;18:53
(b) Mizushima N, Levine B, Cuervo AM, Klionsky DJ. Autophagy fights disease through cellular selfdigestion. *Nature.* 2008;451:1069–1075
(c) Lavandero S, Troncoso R, Rothermel BA, Martinet W, Sadoshima J, Hill JA. Cardiovascular autophagy: concepts, controversies, and perspectives. *Autophagy.* 2013;9:1455–1466.
27. (a) Mizushima N, Yoshimori T, Levine B. Methods in mammalian autophagy research. *Cell.* 2010;140:313–326
(b) Ichimura Y, Kumanomidou T, Sou YS, et al. Structural basis for sorting mechanism of p62 in selective autophagy. *J Biol Chem.* 2008;283:22847–22857.
28. (a) Fekrmandi F, Wang TT, White JH. The hormone-bound vitamin D receptor enhances the FBW7-dependent turnover of NF-κB subunits. *Sci Rep.* 2015;5:13002
(b) Singh PK, van den Berg PR, Long MD, et al. Integration of VDR genome wide binding and GWAS genetic variation data reveals co-occurrence of VDR and NF-κB binding that is linked to immune phenotypes. *BMC Genomics.* 2017;18:132
(c) Griffin MD, Dong X, Kumar R. Vitamin D receptor-mediated suppression of RelB in antigen presenting cells: a paradigm for ligand-augmented negative transcriptional regulation. *Arch Biochem Biophys.* 2017;460:218–226
(d) Chen Y, Zhang J, Ge X, Du J, Deb DK, Li YC. Vitamin D receptor inhibits nuclear factor κB activation by interacting with IκB kinase β protein. *J Biol Chem.* 2013;288:19450–19458.
29. (a) Wu S, Liao AP, Xia Y, et al. Vitamin D receptor negatively regulates bacterial-stimulated NF-κB activity in intestin. *Am J Pathol.* 2010;177:686–697
(b) Won S, Sayeed I, Peterson BL, Wali B, Kahn JS, Stein DG. Vitamin D prevents hypoxia/reoxygenation-induced blood-brain barrier disruption via vitamin D receptor-mediated NF-kB signaling pathways. *PLoS ONE.* 2015;10:e0122821
(c) Chen YH, Yu Z, Fu L, et al. Vitamin D3 inhibits lipopolysaccharide-induced placental inflammation through reinforcing interaction between vitamin D receptor and nuclear factor kappa B p65 subunit. *Sci Rep.* 2015;5:10871
(d) Sun B, Gao L, Ahsan A, et al. Anticancer effect of SZC015 on lung cancer cells through ROS-dependent apoptosis and autophagy induction mechanisms in vitro. *Int Immunopharmacol.* 2016;40:400–409
(e) Ji Q, Sun Z, Yang Z, et al. Protective effect of ginsenoside Rg1 on LPS-induced apoptosis of lung epithelial cells. *Mol Immunol.* 2019. https://doi.org/10.1016/j.molimm.2018.11.003
(f) Gao L, Wang Y, Xu Z, et al. SZC017, a novel oleanolic acid derivative, induces apoptosisand autophagy in human breast cancer cells. *Apoptosis.* 2015;20:1636–1650.